NONLINEAR MODEL PREDICTIVE CONTROL SOLUTION FOR A HYBRID LIFE SUPPORT SYSTEM

Dharmashankar Subramanian and Nitin Lamba

Honeywell Laboratories.
3660, Technology Drive, Minneapolis, MN 55418 USA
{dharmashankar.subramanian, nitin.lamba}@honeywell.com

Abstract: We consider the control problem of a Variable Configuration CO_2 Removal system, which exhibits a hybrid dynamical character due to various operating modes of the system. The objective of the control problem is to track a desired concentration profile of CO_2 and O_2 in a crew cabin while keeping their concentrations within permissible bounds. We present a novel adaptation of the model predictive control technique for a nonlinear hybrid dynamic system. We exploit the problem structure and map the hybrid optimization problem onto a continuous nonlinear program. We also discuss case studies showing controller performance during off-nominal conditions.

Keywords: nonlinear control, optimal control, predictive control, hybrid modes, mathematical programming.

1. INTRODUCTION

Hybrid dynamic models describe hierarchical processes, which evolve according to different sets of lower level dynamic components (differential or difference equations) depending on the upper level logical/discrete mode that characterizes the system, at any given point in time. Hybrid systems have many applications and many approaches to develop control schemes for them exist. The goal of this work is to investigate approaches that may be of practical use to a broad class of hybrid problems. The specific application domain for this work is advanced life support systems that are used for manned space exploration missions. In particular, we consider the control problem of a Variable Configuration CO_2 Removal (VCCR) system, which exhibits a hybrid dynamical character due the various configurations/modes in which one could operate the system. The VCCR is part of an overall Air Recovery System (Finn, 1999; Malin, *et al.*, 2000), which in turn is part of an intended human life-support system for space exploration. The paper is organized as follows: Section II presents the configuration and hybrid dynamic model of the VCCR system, Sections III and IV present the nonlinear model predictive control synthesis, and Section V presents simulation results.

2. VARIABLE CONFIGURATION CO_2 REMOVAL

2.1 System Description

The basic functions of the VCCR system include recovery of CO_2 from the crew cabin by adsorption into one of two adsorber beds. It also includes desorbing the accumulated CO_2 and sending it to an accumulator for downstream CO_2 Removal System (CRS). In this study, we look at a physical idealization of the VCCR system (the configuration of which was obtained from Metrica Traclabs) that consists only of the crew cabin, two adsorber beds, and the CO_2 accumulator, without the CRS system, as shown in Figure 1.

The physical configuration of the system is such that when one of the adsorber beds is connected to the crew cabin, and is undergoing CO_2 uptake via adsorption, the other bed is undergoing either air-save or desorption, with the following synchronized operation. During the time interval (say, 'half-cycle') when the adsorbing bed returns CO_2-lean air back into the cabin, the other bed involves two modes of operation in sequence - the Air-Save mode and the CO_2-desorb mode. In Air-save mode, the desorbing bed recycles CO_2-lean air back into the cabin from its gas phase. For the remainder of the 'half-cycle', it operates in the CO_2-desorb mode in which it delivers CO_2 that is released from the solid phase. This CO_2 can either be vented, or be accumulated into the CO_2 accumulator. During maintenance, the accumulator can also be used to send CO_2 back into the cabin, if needed. The adsorber beds have a saturation capacity beyond which they cannot adsorb any more CO_2. As a result, after every adsorption step, the beds change their roles and the adsorbing bed starts air-save followed by desorption, while the re-generated bed is connected to the cabin for adsorption. Lastly, the overall system has an oxygen generation system (OGS), which can send make-up O_2 into the cabin, if required. Therefore, the system is operated in a cyclical pattern of operation. At any given point in time, the system can exist in any of four different hybrid modes, which form a sequence of four quarter-cycles that compose one full-cycle of operation.

- Mode 1: Bed 1 in Adsorb, Bed 2 in Air-Save.
- Mode 2: Bed 1 in Adsorb, Bed 2 in Desorb.
- Mode 3: Bed 2 in Adsorb, Bed 1 in Air-Save.
- Mode 4: Bed 2 in Adsorb, Bed 1 in Desorb.

The dynamic equations that describe the state evolution in the adsorber beds, crew cabin, and the CO_2 accumulator are different, depending on what mode of operation applies to the system. These are detailed in Subramanian, *et al.*, 2004, and are not repeated here.

3. NON LINEAR MODEL PREDICTIVE CONTROL

Controller synthesis with mathematical programming is based on the so-called receding horizon philosophy. Traditionally (Morari and Lee, 1999; Bemporad and Morari, 1999), this has been done on linear dynamic hybrid systems, and is also referred to as Model Predictive Control (MPC). We have adapted this concept to work with nonlinear, hybrid systems, and call it nonlinear model predictive control (NMPC) in the rest of the paper. A good overview of nonlinear model predictive control can be found here (Henson and Seborg, 1997). The permissible modes of operation of the system and the cyclical pattern of these modes are noted in this section, from the perspective of developing a nonlinear programming based controller.

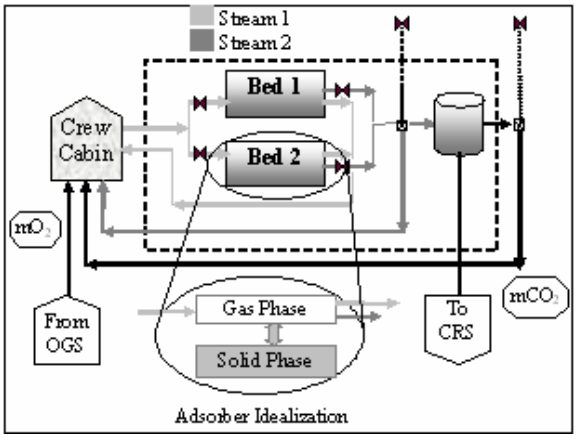

Fig. 1. VCCR Model.

For a given number of full-cycles under consideration, the control inputs to be decided by any controller include the following for each quarter cycle:

1. Volumetric flow rate, v_1
2. Volumetric flow rate, v_2
3. Time duration of each quarter cycle
4. CO_2 Mass flow rate from accumulator to cabin.
5. Mass flow rate of O_2 from the OGS to the cabin

In traditional linear MPC and NMPC, the continuous time axis is discretized into a discrete number of time points, and the differential equations are converted into difference/algebraic equations applied at these time points. The number of time points denotes the regulation horizon over which the classical MPC problem is formulated. Our adaptation of this concept in the NMPC framework for the VCCR physical system is as follows.

We define our NMPC regulation horizon at the time scale of quarter cycles, i.e. a finite number of quarter cycles into the future. This is a subtle, and novel, departure from classical MPC, where the control regulation horizon is defined in terms of the number of discretization points. Within each quarter cycle, the NMPC framework utilizes an appropriate nonlinear model of the system to predict the future state. We use collocation on finite elements (Ascher and Petzold, 1998; Biegler, *et al.*, 2002) to convert the infinite dimensional, continuous, differential equations into a finite dimensional, discretized set of algebraic equations within each quarter cycle (see Figure 2). Based on prediction done over the regulation horizon, a future optimal control maneuver is computed for each quarter cycle in the horizon, in terms of the control inputs noted previously. The control inputs that are actually implemented correspond to the first quarter cycle.

The details of the nonlinear programming formulation within the NMPC framework are described next. Firstly, the time axis is modeled into a specified number of quarter-cycles along with some set definitions (Table 1) that aid in converting a set of four mode-dependent *sets* of dynamic equations into a single finite-dimensional set of discretized

algebraic equations. Let $I=\{i_0, i_0+1,..., i_0+G-1\}$, where G is the number of quarter-cycles under consideration (i.e. the NMPC regulation horizon, as adapted for our work). The system can start with any mode, with the only restriction that the two beds follow the cyclical pattern for subsequent quarter-cycles. Further, let $m=\{i \bmod 4\} \quad \forall i \in I$ to define subsets of I (Table 1) based on the cyclical pattern of operation. These sets exploit the cyclic nature of the process and identify the correct set of differential equations that apply to each quarter cycle in the regulation horizon.

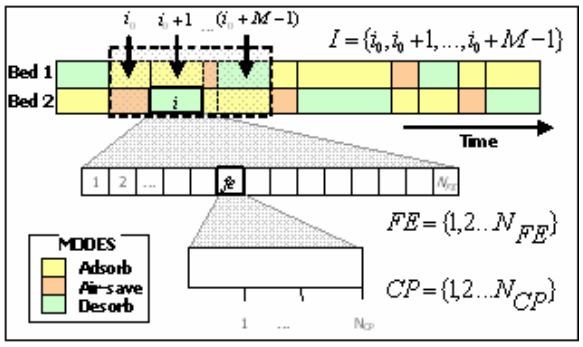

Fig. 2. Time Discretization Schematic.

Table 1 Set Definitions

Bed	Mode	Definition
1	Adsorb	$B_{A,1}=\{i \mid (m=1)\vee(m=2)\}$
2	Adsorb	$B_{A,2}=\{i \mid (m=3)\vee(m=0)\}$
1	Air-Save	$B_{AS,1}=\{i \mid (m=3)\}$
2	Air-Save	$B_{AS,2}=\{i \mid (m=1)\}$
1	Desorb	$B_{D,1}=\{i \mid (m=0)\}$
2	Desorb	$B_{D,2}=\{i \mid (m=2)\}$
1,2	Adsorb	$B_A=\{(i,j) \mid [(j=1)\wedge(i\in B_{A,1})] \vee [(j=2)\wedge(i\in B_{A,2})]\}$
1,2	Air-Save	$B_{AS}=\{(i,j) \mid [(j=1)\wedge(i\in B_{AS,1})] \vee [(j=2)\wedge(i\in B_{AS,2})]\}$
1,2	Desorb	$B_D=\{(i,j) \mid [(j=1)\wedge(i\in B_{D,1})] \vee [(j=2)\wedge(i\in B_{D,2})]\}$

For each quarter cycle, *i*, the time interval of interest, *T(i)*, which is the same of the (unknown) duration of the quarter cycle, is divided into N_{FE} finite elements of length h_{fe}, such that

$$\sum_{fe=1}^{fe=N_{FE}} h_{fe} = T(i) \tag{1}$$

We have taken the finite elements to be of equal size. If the time duration, *T(i)*, is represented by the interval $[t_{i,0}, t_{i,f}]$, then,

$$t_{i,fe} = t_{i,0} + \sum_{l=1}^{l=fe} h_l, \forall fe = 1,.., N_{FE} \qquad (note: t_{i,N_{FE}} = t_{i,f}) \tag{2}$$

Within each finite element, we place N_{CP} collocation points. The time profiles of algebraic and differential variables are approximated using derivatives and values evaluated at the N_{CP} collocation points, whose relative position within each finite element is the same. The collocation points are positioned as,

$$t_{i,fe,cp} = t_{i,fe-1} + h_{fe}\lambda_{cp}, \forall cp = 1,..., N_{CP} \tag{3}$$

In the above equation, $\lambda_{cp} \in [0,1]$, and are chosen to be the shifted roots of orthogonal polynomials of degree N_{CP}. In this work, we use Radau points, as they allow convenient setting of constraints at the end of each element (Bader and Ascher, 1987). A monomial basis representation is used for the differential profiles. So a differential variable, *z*, in quarter cycle, *i*, and finite element, *fe*, is given as:

$$z_i(t) = z_{i,fe-1} + h_{fe}\sum_{cp=1}^{N_{CP}} \Omega_{cp}\left(\frac{t-t_{i,fe-1}}{h_{fe}}\right)\left(\frac{dz_i}{dt}\right)_{i,fe,cp} \quad \forall t \in [t_{i,fe-1}, t_{i,fe}] \tag{4}$$

In the above equation, the time polynomial Ω_{cp} is of order N_{CP}, and uniquely satisfies the following conditions:

$$\Omega_{cp}(0)=0, \text{ for } cp=1,...,N_{CP}$$
$$\Omega'_{cp}(\rho_k)=\delta_{q,k}, \text{ for } cp=1,...,N_{CP}; k=1,...,N_{CP} \tag{5}$$

The ODEs are written at each collocation point with each finite element by introducing a variable for each state-derivative. Continuity constraints are imposed at the boundaries of each finite element, and at the boundaries of each quarter cycle time slot.

4. NLP FORMULATION

4.1 System Constraints

Let $M=\{CO_2, O_2, inert\}$ be the set of components in the system, and $J=\{1,2\}$ be the set representing the two beds in the system. Also, let subscript *C* denotes the crew cabin, and subscript *A* denotes the CO_2 accumulator. Symbol definitions are given in the Appendix.

$$V_C\left(\rho_C^{Gra}(c,i,fe,cp)\right) = \left[\begin{array}{l} v_1(i)\left(\rho(c,i,j,fe,cp) - \rho_C(c,i,fe,cp)\right) \\ + r_C(c) + v_2(i)\rho(c,i,j',fe,cp) + \dot{m}(i,c) \end{array}\right] \tag{6}$$
$$\forall i \in I,\ fe \in FE,\ cp \in CP, c \in M,$$
$$(i,j,j') \mid \left(j \neq j', \&(i,j) \in B_A, \&(i,j') \in B_{AS}\right).$$

$$V_C\left(\rho_C^{Gra}(c,i,\ fe,cp)\right)=\begin{bmatrix} v_1(i)\begin{pmatrix}\rho(c,i,\ j,\ fe,cp)\\ -\rho_C(c,i,\ fe,cp)\end{pmatrix}\\ +r_C(c)+\dot{m}(i,c)\end{bmatrix} \quad (7)$$

$$\forall i \in I,\ fe\in FE,\ cp\in CP, c\in M,$$
$$(i,\ j,\ j')\big|\ j\neq j', \&(i,\ j)\in B_A, \&(i,\ j')\in B_D.$$

The discretized sets of algebraic equations transform the differential equations into constraints that represent the dynamics in the NLP formulation. The crew cabin material balance in the Air-Save and Desorb mode respectively take the above form upon discretization.

The adsorber bed material balances in the Adsorb mode take the following form upon discretization:

$$V_j\rho^{Gra}(c,i,\ j,\ fe,cp)=\begin{bmatrix} v_1(i)\begin{pmatrix}\rho_C(c,i,\ fe,cp)\\ -\rho(c,i,\ j,\ fe,cp)\end{pmatrix}\\ -r_{ads}(j,c)\end{bmatrix} \quad (8)$$

$$\forall i \in I,\ fe\in FE,\ cp\in CP, c\in M,\ (i,\ j)\in B_A$$

$$Q^{Gra}(c,i,\ j,\ fe,cp)=r_{ads}(j,c)$$
$$\forall i \in I,\ fe\in FE,\ cp\in CP, c\in M, (i,\ j)\in B_A \quad (9)$$

Similar discretization is done for the adsorber bed material balances in the Air-Save and Desorb modes, using sets B_{AS} and B_D. The accumulator material balances in the Air-Save and Desorb mode respectively take the following form upon discretization:

$$Q_A^{Gra}(c,i,\ fe,cp)=-\dot{m}(i,c)$$
$$\forall c=CO_2,\ fe\in FE,\ cp\in CP, \quad (10)$$
$$\forall i\in I,\ j\big|\ (i,\ j)\in B_{AS}$$

$$Q_A^{Gra}(c,i,\ fe,cp)=-\dot{m}(i,c)+v_2(i)\rho(c,i,\ j,\ fe,cp)$$
$$for\ c=CO_2, \forall i\in I,\ fe\in FE, cp\in CP, (i,\ j)\in B_D \quad (11)$$

The mass fraction of every component in the crew cabin is defined with the following constraint:

$$y_C(c,i,\ fe,cp)\sum_{c'\in C}\rho_C(c',i,\ fe,cp)=\rho_C(c,i,\ fe,cp)$$
$$\forall i\in I,\ fe\in FE,\ cp\in CP, c\in M \quad (12)$$

The constraints that model the continuity conditions across the quarter-cycle time slots in the discretized model are as follows:

$$\rho_C^0(c,i,1)=\rho_C(c,i-1,N_{FE},N_{CP})$$
$$\forall\ i\in I\ |\ i\ >i_0, c\in M \quad (13)$$

To determine variable values at every collocation point within finite elements, following constraints are obtained:

$$\rho_C(c,i,\ fe,cp)=\rho_C^0(c,i,\ fe)$$
$$+\frac{T(i)}{N_{FE}}\sum_{cp'=1}^{N_{CP}}\Omega(cp',cp)[\rho_C^{Gra}(c,i,\ fe,cp')] \quad (14)$$
$$\forall i\in I,\ fe\in FE,\ cp\in CP, c\in M$$

Similarly, the constraints that model the continuity conditions across finite elements take the following form:

$$\rho_C^0(c,i,\ fe)=\rho_C^0(c,i,\ fe-1)$$
$$+\frac{T(i)}{N_{FE}}\sum_{cp'=1}^{N_{CP}}\Omega(cp',N_{CP})[\rho_C^{Gra}(c,i,\ fe,cp')] \quad (15)$$
$$\forall i\in I,\ fe\in FE\ |\ fe>1,\ c\in M$$

Similar constraints are imposed for variables, $Q_A(c,i,\ fe,cp)$, $\rho(c,i,\ j,\ fe,cp)$ and $Q(c,i,\ j,\ fe,cp)$.

Additionally, the length of time slot was also bounded by appropriate values to avoid getting trivial solutions (with zero length of time slots). Lastly, at the end of air-save step, pure vacuum cannot be attained and the bed fluid phase can only reach a certain minimum pressure. So we define a minimum total concentration corresponding to that attainable pressure. Moreover, in order to prevent loss of oxygen and inert into the CO_2 accumulator, a maximum total concentration is also defined. The system parameters, physical bounds and nominal initial conditions are described in these papers (Subramanian *et al*. 2004, and Glavaski, 2004).

4.2 Objective Function

The classical objective function used in linear and nonlinear MPC is reference state trajectory tracking. For complex, hybrid systems, such as the subject of study in this paper, such an objective function may not be sufficient to address the desired trade-off between long-term nominal stability and short horizon of control calculation. We used a systematic procedure to develop an appropriate objective function, which is expressed as a weighted sum of six measures corresponding to the following six goals:

1. CO_2 control: follow CO_2 set point in the cabin.
2. O_2 control: follow O_2 set point in the cabin.
3. Chattering control: avoid excessive switching.
4. Desorption driver: allow sufficient desorption.
5. CO_2 driver: drive CO_2 out of the bed fluid phase.
6. Low Bed CO_2 driver: maintain low solid phase loading (of CO_2) by the end of the desorb mode.

The details of this development are described in this paper (Subramanian *et al*. 2004). Consequently, the NMPC objective, which provides good long-term performance, takes the following form:

Minimize

$$w_1\sum_{i\in I}\sum_{fe\in FE, cp\in CP}\left(y_C(CO_2,i,\ fe,cp)-y_C^*(CO_2)\right)^2$$
$$+w_2\sum_{i\in I}\sum_{fe\in FE, cp\in CP}\left(y_C(O_2,i,\ fe,cp)-y_C^*(O_2)\right)^2$$
$$-w_3\sum_{i\in I}T(i)$$
$$+w_4\sum_{c=CO_2}\sum_{(i,j)\in B_D}Q(c,i,\ j,N_{FE},N_{CP})-Q^0(c,i,\ j) \quad (16)$$
$$-w_5\sum_{c=CO_2}\sum_{(i)\in I_D}Q_A(c,i,N_{FE},N_{CP})$$
$$+w_6\sum_{c=CO_2}\sum_{(i,j)\in B_D}Q(c,i,\ j,N_{FE},N_{CP})$$

Thus, the multi-objective NLP formulation is defined as: Objective (16) subject to all the discretized algebraic equations, like (6)-(15), and physical bounds on control inputs.

5. SIMULATION RESULTS

5.1 Controller Tuning

The multi-objective NLP optimization formulation requires tuning of the weights for the six terms that occur in the objective function. The tuning exercise was carried out in two steps: first, taking into account the typical magnitudes of the contributions of the six terms to the objective, and then, factoring the relative importance of these goals. The CO_2 concentration control was chosen as the most important, and controller chattering was chosen as the least important goal. The performance of the controller with the tuned weights has been studied in a case study with a nominal initial condition of the system. The system parameters, physical bounds, nominal initial conditions and tuned weights of objective terms are described in Subramanian *et al*. (2004).

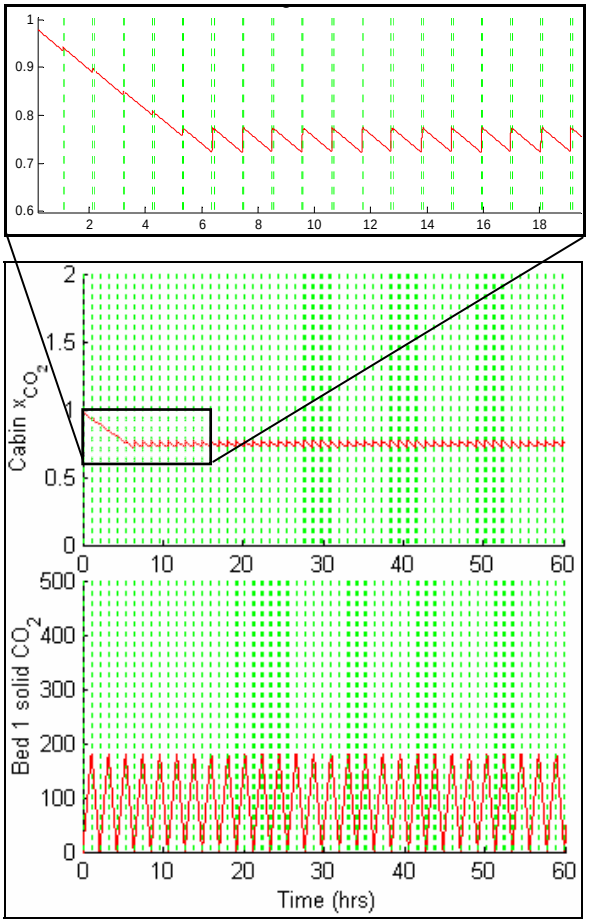

Fig 3: NMPC Controller Performance with High Initial CO2 in the Crew Cabin.

The *baseline* tuning of weights gives good performance on all six objectives. An important point to note here is that the NLP has feasibility embedded within its formulation as a set of hard constraints. In the presence of desirable terms in the objective, say low bed CO_2 driver term, the controller seeks qualitatively better solutions, in addition to just feasibility – in this case, ability to maintain low average CO_2 levels in bed solid phase to have long, stabilized, cycle-times and accommodate future eventuality.

5.2 Case Studies

We present the controller performance on two off-nominal conditions:

1. Cabin at very high CO_2 concentration
2. Cabin at very low CO_2 concentration

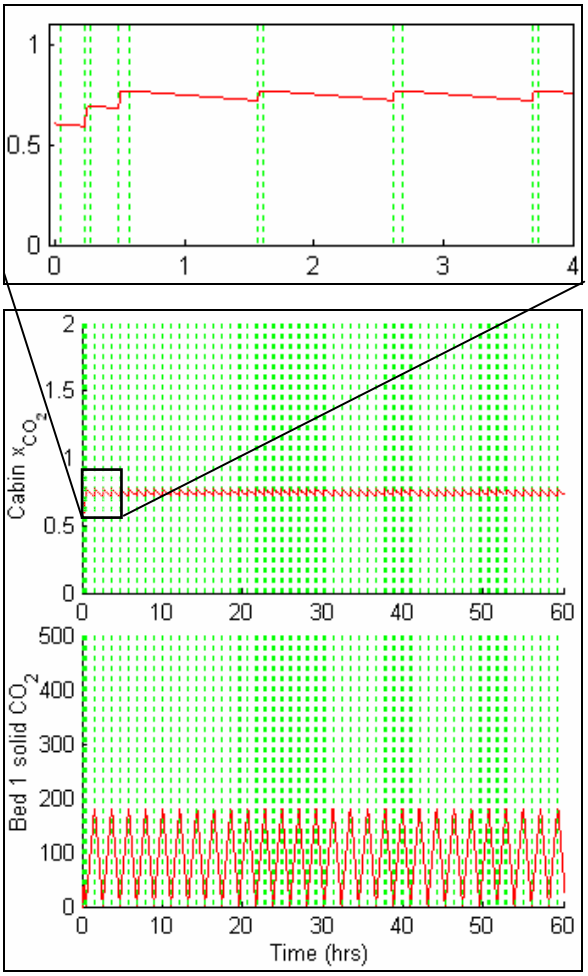

Fig 4: NMPC Controller Performance with Low Initial CO2 in the Crew Cabin.

The primary goal was to study the effect of such extreme scenarios on the performance of the controller. The NLP optimization formulation was modeled using AMPL (Fourer *et al*., 1993) and solved using CONOPT. This NLP model (the controller) was coupled with a MATLAB model of the VCCR system (the simulator) so that the control actions obtained after solving the NLP model could be used to simulate the system in time. For these two cases, the VCCR-NMPC system was simulated for about 160 hours, indicating good nominal stability

and performance. The NLP corresponding to any single prediction horizon was solved in ~ 3 minutes, on a Windows Desktop with 1GB RAM, and Pentium IV, 1.5 GHz processor.

Figures 3 and 4 show the carbon dioxide concentration (in % mass fractions) profiles for the two cases. It takes the cabin CO_2 concentrations to the desired set-point and maintains it around the set-point. A stable cyclic pattern is observed in solid phase concentration of both adsorber beds with 5 minute air-save mode and 1 hour desorb mode. Thus, the NMPC demonstrates effective controller performance in the face of off-nominal initial concentrations in the cabin.

6. CONCLUSIONS

We have described an adaptation of MPC for a nonlinear, hybrid dynamic system. The proposed technique views the NMPC horizon in units of time-intervals that the system spends in various hybrid modes, and applies collocation on finite elements to describe the evolution of the nonlinear dynamic system within each time-interval (mode). Such a view appears general enough to address a broad class of nonlinear hybrid systems, which exhibit a structured pattern of switching across modes.

ACKNOWLEDGMENT

This work was funded by NASA Ames Research Center, under Contract # NAS2-01067. The authors thank Dr. Robert Morris, NASA Ames Research Center, as well as Sonja Glavaski, Ranjana Deshpande and Kartik Ariyur, Honeywell Labs, for their input and support.

APPENDIX

Notation: Variables

1. Adsorber Beds:

$\rho(c,i,j,fe,cp)$	Fluid phase concentration at cp within fe.
$\rho^0(c,i,j,fe)$	Fluid phase concentration at the start of fe.
$\rho^{Gra}(c,i,j,fe,cp)$	Gradient of fluid phase concentration.
$Q(c,i,j,fe,cp)$	Solid phase mass at *cp* within *fe*.
$Q^0(c,i,j,fe)$	Solid phase mass at the start of *fe*.
$Q^{Gra}(c,i,j,fe,cp)$	Gradient of mass accumulation.

2. Cabin

$\rho_C(c,i,fe,cp)$	Component concentration at cp within *fe*.
$\rho_C^0(c,i,fe)$	Component concentration at the start of *fe*.
$\rho_C^{Gra}(c,i,fe,cp)$	Gradient of concentration at *cp* within *fe*.
$y_C(c,i,fe,cp)$	Component mass fraction at *cp* within *fe*.

3. Accumulator

$Q_A(c,i,fe,cp)$	Component mass at *cp* within *fe*.
$Q_A^0(c,i,fe)$	Component mass at the start of *fe*.
$Q_A^{Gra}(c,i,fe,cp)$	Gradient of component mass.

4. Streams

$v_1, v_1(i)$	Flow rate from the cabin to adsorbing bed, in *i*.
$v_2, v_2(i)$	Flow rate from air-saving or desorbing bed, in *i*.
$\dot{m}(c), \dot{m}(i,c)$	Component mass flow rate, in *i*.

5. Time

$T(i)$	Time duration of time slot *i*.

Notation: Parameters

$r_C(c)$	Rate of generation in the crew cabin.
$r_{ads}(j,c)$	Rate of adsorption in bed *j*.
$r_{des}(j,c)$	Rate of desorption in bed *j*.
V_j	Fluid phase volume of bed *j*.
V_C	Crew cabin volume.
$\Omega(cp,cp')$	Multipliers for Cubic Roots (for collocation).

REFERENCES

Ascher, U.M. and Petzold, L.R. (1998). *Computer Methods for Ordinary Differential Equations and Differential-Algebraic Equations*, SIAM, Philadelphia, PA, USA

Bader, G., and Ascher, U. (1987). A new basis implementation for mixed order boundary value ODE solver. *SIAM J. Scientific Computing*, **Vol. 8**, No. 4, pp. 483

Bemporad, A., Morari, M. (1999). Control of Systems integrating logic, dynamics, and constraints. *Automatica*, **35**, pp. 407-427.

Biegler, L. T., Cervantes A. and Waechter, A. (2002). Advances in Simultaneous Strategies for Dynamic Process Optimization. *Chemical Engineering Science*, **57**, pp. 575-593.

CONOPT solver by ARKI Consulting & Development A/S http://www.conopt.com

Finn, C. (1999). *Documentation of the BIO-Plex Baseline Simulation Model*, NASA Ames Research Center.

Fourer, R., Gay, D., and Kernighan, B. (1993). *AMPL*, The Scientific Press, South San Francisco, California.

Glavaski, S. (2004). Automatically Synthesizing Guaranteed Hybrid Controllers For Adaptive Autonomous Systems (ASHC). *Annual Report submitted to NASA-Ames Research Center under Contract Number NAS2-01067*.

Henson, M. A. and Seborg, D. E. (1997). *Nonlinear process control*, Prentice Hall, Upper Saddle River, New Jersey.

Malin, J., Kowing, J., Schreckenghost, D.,Bonasso, P., Nieten, J., Graham, J., Fleming, L., MacMahon, M., Thronesbery, C. (2000). Multi-Agent Diagnosis and Control of an Air Revitalization System for Life Support in Space. *Proceedings of the IEEE Aerospace Conference*.

Morari, M. and Lee, J. H. (1999). Model Predictive Control: Past, Present and Future. *Comp. Chem. Engg*., **23 (4-5)**, pp. 667-682.

Subramanian, D., Lamba, N., Ariyur, K., Deshpande, R., and Glavaski, S. (2004). Predictive Control of a Nonlinear Hybrid Life Support System. Submitted to *IEEE Trans. Control Systems Technology*.